Lower-extremity musculoskeletal geometry affects the calculation of patellofemoral forces in vertical jumping and weightlifting.

Cleather, Daniel J. and Bull, Anthony M. J. (2010) *Lower-extremity musculoskeletal geometry affects the calculation of patellofemoral forces in vertical jumping and weightlifting.* Proceedings of the Institution of Mechanical Engineers, Part H: Journal of Engineering in Medicine, 224 (9). pp. 1073-1083. ISSN 0954-4119

Version: Post-print

Official link e.g. http://dx.doi.org/10.1243/09544119JEIM731

Lower Extremity Musculoskeletal Geometry Effects the Calculation of Patellofemoral Forces in Vertical Jumping and Weightlifting

Daniel J Cleather[1] and Anthony MJ Bull[2]

[1] School of Human Sciences, St Mary's University College and Department of Bioengineering, Imperial College London

[2] Department of Bioengineering, Imperial College London

Keywords: musculoskeletal modelling, inverse dynamics, optimisation, patellofemoral force, jumping

Daniel Cleather,

St. Mary's College,

Waldegrave Road,

Twickenham.

TW1 4SX

UK

Tel: +44 7973 873 516

Email: dancleather@hotmail.com

Abstract

The calculation of patellofemoral joint contact force using three dimensional (3-D) modelling techniques requires a description of the musculoskeletal geometry of the lower limb. In this study, the influence of the complexity of the muscle model was studied by considering two different muscle models, the Delp and Horsman models. Both models were used to calculate the patellofemoral force during standing, vertical jumping and Olympic style weightlifting. The patellofemoral forces predicted by the Horsman model were markedly lower than those predicted by the Delp model in all activities and represented more realistic values when compared to previous work. This was found to be a result of a lower level of redundancy in the Delp model, which forced a higher level of muscular activation in order to allow a viable solution. The higher level of complexity in the Horsman model resulted in a greater degree of redundancy and consequently lower activation and patellofemoral forces. The results of this work demonstrate that a well posed muscle model must have an adequate degree of complexity to create a sufficient independence, variability and number of moment arms in order to ensure adequate redundancy of the force sharing problem such that muscle forces are not overstated.

Keywords: musculoskeletal modelling, muscle models, musculoskeletal geometry, patellofemoral joint force

1. Introduction

Musculoskeletal modelling techniques can be used to analyse biomechanical problems where the direct measurement of key variables is difficult or impossible. This requires a detailed description of the geometry of the musculoskeletal system to allow the calculation of muscle lines of action and moment arms. A large number of previous authors have employed this methodology to solve problems of biomechanical interest (e.g. [1]-[7]).

The Delp muscle model of the lower limb [8]-[10] has been used in a large number of studies to describe the geometry of the lower limb [11], [12]. This muscle model is an amalgamation of previous studies [13]-[15] that has been widely altered and refined since its inception (e.g. [16], [17]). Horsman et al [18] have recently published a complete data set which is, for the first time, based on the geometrical analysis of one cadaveric specimen [18]. The use of one cadaveric specimen has the advantage of ensuring internal consistency within the data set while at the same time being limited in the extent to which it can be assumed to be representative of the wider population. Within both models line elements are specified to describe the line of action of the muscles, however, the model of Horsman is considerably more detailed than that of Delp as it includes almost four times as many line elements.

Patellofemoral joint problems affect a large number of individuals [19] and are likely to be related to the contact forces and stresses experienced at the joint [20], [21]. A number of 2 and 3-D models (e.g. [20]-[24]) have been employed to study patellofemoral joint contact force during movement and the calculated forces range from 0.4 *kN* during walking [21], [22] to 6.0 *kN* when landing after a jump [24].

The purpose of this study was to analyse the effect of the choice of muscle model on the analysis of movement in a problem of clinical significance that is, the calculation of patellofemoral joint contact force, by comparing the application of two different muscle models. In particular, the aim of the study was to explore the merits of using more complex and detailed models in musculoskeletal modelling. The Delp model was chosen due to its wide use in musculoskeletal modelling research. The original Delp model was employed because of the difficulties in presenting a modified Delp model that included all of the refinements in the literature and as it represented a less complex and refined model. The Horsman model was chosen as the second model as it represents the first muscle model that has been created solely by reference to one source, and due to the fact that it represents a more complex and refined model that is still based upon a very similar methodology to the Delp model. The aim was to provide an analysis of the differences between these data sets in terms of modelling parameters, assumptions and clinical results, and to highlight some of the key general considerations when employing muscle models in these types of analyses.

2. Methods

This study employed a 3-D musculoskeletal model of a right lower limb. The function of the model used in this paper is described in Figure 1 and in detail below. In summary, inverse dynamics was used to calculate joint forces and moments during standing, vertical jumping and weightlifting (jerking a 40 *kg* barbell overhead). The two muscle models were used to calculate individual muscle forces using optimisation techniques. Finally, the musculoskeletal geometry and muscle forces were combined to calculate the patellofemoral joint contact force. The data was for a 33 year old, physically active male (height 1.86 *m*, mass 85.0 *kg*).

Figure 1 about here.

The model employed in this paper was verified by comparison with previously published musculoskeletal models of this type. In particular, the intersegmental analysis of jumping calculated by the model was compared to previous work [25], [26]. Similarly, the patellofemoral joint contact force calculated by the model during various tasks was compared to the work of previous authors. The model was found to be in good agreement with previous models and was thus considered to be appropriate for employment in this study.

2.1 Inverse Dynamics

Optical motion tracking was used to collect lower limb kinematics where the standard marker placements of Van Sint Jan et al [27] were used to locate key anatomical landmarks [27], [28]. Force data was recorded using a force plate (Kistler Type 9287, Kistler Instrumente AG, Winterthur, Switzerland) and synchronised with the motion capture data (Vicon MX System, Vicon Motion Systems Ltd, Oxford, UK). The subject performed the activities with only one foot on the force plate in order to

record measurements that were consistent with the specification of a single right lower limb model. The model comprised four linked rigid segments and is illustrated in Figure 2. The marker positions were used to calculate the transformation specifying the location and orientation of the rigid bodies representing the foot, lower leg, thigh and pelvis segments [29]. The segments were considered to meet at the centre of rotation (COR) of each joint as defined by each muscle model in relation to anatomical landmarks and the particular muscle model used (i.e. the Delp model [8]-[10] or the Horsman model [18]) and the COR was considered to be fixed within the distal segment. These assumptions limit the joints to purely rotational movement and discount any translation at the joints. The transformation specifying the location and orientation of each segment was smoothed using linear time-invariant and quaternion filtering techniques as described by Lee and Shin [30].

Figure 2 about here.

An inverse dynamics analysis was performed to calculate the intersegmental forces and moments at each joint of the model during the movement using the Newton-Euler iterative method as described by Winter [31]. This method is based upon the fact that if the force and moment at the distal end of a kinetic chain is known then classical mechanics can be used to calculate the forces and moments at each joint in a stepwise fashion moving proximally along the kinetic chain. Forces were calculated by consideration of the free body diagram of each segment, iteratively, moving proximally along the kinetic chain. The moments at each joint were then found by employing Euler's equations of 3-D motion for a rigid body sequentially, again by moving proximally along the lower limb. In order to employ the Euler equations most efficiently this calculation was performed in the local coordinate system (LCS)

of each segment. This calculation is depicted in Figure 3. Anthropometric data, including segment masses, location of segment centre of masses and segment radii of gyration were taken from de Leva [32].

Figure 3 about here.

2.2 Implementation of the Muscle Models

The muscle models analysed in this paper consist of a description of the geometry of the musculoskeletal system for one specific subject and one posture (the anatomical position). The muscle models are specified by line elements representing the path of each musculotendinous unit including the origin and insertion of each muscle, wrapping over underlying structures, the physiological cross-sectional areas of the muscles and a description of the spatial relationship between the patella and femur. No passive tissues were modelled in the study.

In order to generalise the muscle model to any given posture a body fixed LCS was created for each of the rigid body segments specifying the model and all muscle geometry was expressed within these LCSs. A transformation was calculated from the LCSs to the laboratory fixed global coordinate system (GCS) for each frame. Given this transformation, the musculoskeletal geometry of any posture in the GCS could be calculated. In this study, the x-axis was defined to be the anterior-posterior axis, the y-axis to be superior-inferior, and the z-axis to be lateral-medial. Subject-specific scaling of the muscle model was achieved at the segmental level. Dividing the length of the subject's segments (as represented by anatomical landmarks) by those of the model allowed the calculation of a linear scaling factor along the longitudinal axes of the segments. The lack of further information as to the dimensions of the Delp segments precluded the calculation of scaling factors along

the other two axes of each segments. The scaling factor was applied to each muscle point in order to calculate the personalised y-coordinate of each muscle point.

2.2.1 Delp Muscle Model

The Delp muscle model has 43 line elements. Wrapping of muscles over underlying structures was achieved by the use of via points. Via points are additional points through which a line element is constrained to pass thus permitting a more detailed description of the path of a muscle. Additional via points were specified for particular joint angles at the knee. The hip was modelled as a joint with 3 degrees of freedom (DOF), the knee with 1 DOF and the ankle with 2 DOF. These constraints are in agreement with the original Delp model and were necessary to allow the optimization to solve. However, in particular, modelling the knee as a 1 DOF joint may be particularly limited given that the extra DOF may be especially useful in understanding the mechanisms of injury. The Delp knee model is specified by the transformation from tibia to patella given a particular knee angle, this relationship is extrapolated from previous research [33]-[35]. The movement of the patella is constrained to patellar rotation in the sagittal plane of the patella relative to the tibia.

2.2.2 Horsman Muscle Model

The Horsman muscle model has 163 individual line elements and includes the position of anatomical landmarks and CORs. In order to express the muscle model in the body fixed segmental LCS, the anatomical landmarks of the Horsman muscle model were used to calculate a body fixed segmental LCS that was defined on the same basis as that of the subject's. A rotation that mapped the LCS of the Horsman data set to the subject's was then calculated, thus enabling a more subject-specific model than the Delp data set. Where the sliding of the muscle over the underlying

structure is constrained, via points were defined to describe the muscle wrapping. Where a free movement of the muscle over underlying structures is possible, a cylinder was fitted to the structure to approximate its geometry. The muscle wrapping around this structure was then computed to minimise the length of the muscle based on the method of Charlton and Johnson [36]. The hip, knee and ankle joints were all modelled with 3 DOF.

The Horsman knee model represents the circular trajectory that best fit the motion of the patella with respect to the femur. The Horsman data consists of the COR of the patella and its axis of rotation. The motion of the patella can then be calculated by assuming that the patella tendon is an inextensible string that drags the patella around this path. The Horsman knee model was scaled to the subject-specific data by using the same scaling methodology as for the muscle points. Similar to the Delp model, the Horsman model was therefore constrained to rotation in the sagittal plane of the patella.

In order to provide a fair comparison to the Delp muscle model a second Horsman muscle model was implemented. In the adjusted muscle model only those muscles that exist in the Delp model were represented (thus the adjusted model had 152 elements) and the model employed the Delp knee.

2.3 Solution of the Force Sharing Problem

The effective line of action (***l***) of each muscle was calculated for each joint upon which a muscle acts by normalising the vector from the most proximal muscle point in the distal segment to the most distal point in the proximal segment. In order to consider the torque effect of each muscle the vector from the COR to the line of action of the muscle to the proximal segment (***r***) was calculated. If F is the magnitude

of the individual muscle force, then the torque created by each muscle about the COR (***T)*** can be expressed as:

$$\boldsymbol{T}=F\boldsymbol{l}\times\boldsymbol{r}$$

The indeterminate problem of finding the individual muscle forces that produce the torques calculated in the inverse dynamics analysis was then solved by optimising the following objective function proposed by Crowninshield and Brand [37], where F_{max} is the magnitude of the maximum possible muscle force and n is the number of muscle line elements. The objective function is based on minimising muscle stress raised to the power n where increasing n defines an optimal solution path that converges on the solution where muscle stress is equal in each force actuator as n approaches infinity. We have found in our model that optimal force sharing can be achieved with n=30 and would consider that in our application this best represents the physiological basis of the cost function (that of maximising muscle endurance).

$$\min_{F_i} f = \sum_{i=1}^{n}\left(\frac{F_i}{F_{\max_i}}\right)^{30}$$

The optimisation was performed subject to the calculated muscle force being less than the product of the physiological cross-sectional area of the relevant muscle multiplied by the maximum muscle stress of 3.139 x 10^5 N/m^2 proposed by Yamaguchi [38]. The physiological cross-sectional areas for all muscles used in the optimisation were doubled in both models to represent the fact that the subject in this study was from an athletic population whereas the cadaveric data on which the muscle models are based was measured from aged subjects, an approach suggested by Yamaguchi [38]. This was the only adjustment to the muscle parameters. The force-length-velocity relationship was not modelled in this study – the upper bound of the muscle force was based purely on the cross-sectional area and did not vary with joint angle. The

fmincon function from the optimisation toolbox of Matlab (version 7.1; The Mathworks, Inc, 2005) was used to perform the optimisation.

2.4 Calculation of patellofemoral joint contact force

The muscle models defined the line of action of all the muscles and tendons acting on the patella. The individual muscle forces contributing to the knee extension moment for each line of action were calculated in the optimisation. The force vectors as a result of muscular actions on the patella were therefore calculated by multiplying these force values with the vectors expressing the line of action of the muscle elements. The line of action of the patella tendon was also provided by the muscle models. The patella was assumed to be constrained to pure rotation in the sagittal plane of the patella by its passive structures. Consequently, the geometrical relationship between the force in each muscle element and the patellar tendon could be evaluated by the assumption of moment and force equilibrium in the sagittal plane of the patella. This allowed the force in the patellar tendon to be calculated and consequently the vector representing the action of the patella tendon on the patella. The resultant force vector calculated by considering all of the muscular and tendinous force vectors acting on the patella was considered to represent the patellofemoral joint contact force by superposition as the influence of patellofemoral joint geometry can be considered to be small as demonstrated by Powers and colleagues [39].

3. Results

The optimisation was able to find a solution for both the Delp and Horsman muscle models with the subject in standing (Table 1). The Delp model required a greater level of activation in the knee extensors and the ankle muscles. The Horsman model exhibited higher levels of activation in the hip muscles, especially in the abductors, adductors and rotators.

Table 1 about here.

The optimisation found a solution for all frames of data for the Horsman muscle model during the jump trial. The Delp muscle model was solvable for hip flexion ranges up to approximately 65 degrees of hip flexion, but not beyond. It has previously been established that the Delp model is not well defined in deep hip flexion ranges [9]. Figure 4 illustrates the number of gluteal muscle elements with hip extension moment arms as a function of hip angle for the two muscle models. The data presented is based on the International Society of Biomechanics convention on the definition of joint coordinate frames [40]. For the Delp muscle model, increasing hip flexion angle results in a diminishing number of potential muscle fibres that can be involved in providing a hip extension moment. Consequently, in deep hip flexion, the hip extension moment-generating capacity of the model is insufficient to provide a solution for the optimisation. In contrast, the Horsman muscle model has an increasing number of moment arms available to the optimisation as hip flexion angle increases. In this application the Delp model failed due to a lack of both hip extension and abduction moment generating capacity in deep hip flexion.

Figure 4 about here.

Figure 5 presents the patellofemoral joint contact force during vertical jumping for the Delp model (where a solution exists) and the Horsman models. At small hip flexion angles the Delp model exhibits a good level of agreement with the Horsman model. However, as the Delp model approaches failure, the patellofemoral joint contact force rapidly becomes much greater than that of the Horsman model.

Figure 5 about here.

A solution was found all models during a 40 *kg* power jerk. Figures 6 and 7 illustrate the patellofemoral joint contact and patellar tendon forces calculated during the jerk. It is apparent that the Horsman model predicted the lowest forces and the forces predicted by the Delp model are markedly higher than those of the Horsman models. The adjusted Horsman predicted higher patellar tendon forces than the Horsman model however the patellofemoral joint contact forces predicted by the two Horsman models were much closer. This difference can be explained by the effect of the difference in patellofemoral joint kinematics used in the two models on the calculation of patellofemoral joint contact force.

Figures 6 and 7 about here.

Table 2 presents a comparison of the patellofemoral and patellar tendon forces in the jump and jerk based upon the Horsman model. In the propulsive phase of the two activities the peak patellofemoral joint contact force in the jerk is greater than in the jump. In contrast, the patellofemoral joint contact force in the jerk catch phase is less than a jump landing. The same pattern is evident for the patellar tendon force.

Table 2 about here.

4. Discussion

This study evaluated the differences in employing two muscle models of differing complexity when exploring a problem of clinical relevance using musculoskeletal modelling techniques. This study demonstrated that both muscle models can be employed successfully to analyse standing and jerking. The Horsman model can also be used to analyse a jumping task. However, the original Delp model considered in this study was unable to cope with vertical jumping as it is not well specified when the hip is in deep flexion.

This paper highlights an interesting facet of musculoskeletal modelling pertaining to the complexity of the muscle model employed. In a simple 3-D model where each muscle spans only 1 DOF, the number of elements required to solve a static optimisation problem is equal to twice the number of DOFs in the model. However, if muscles span multiple DOF the interplay between synergistic and antagonistic muscles increases the complexity of the force sharing problem. This relationship is governed by the nature of the application and the construction of the muscle model - it is straightforward to exemplify a 3-D model which can arrive at a solution with only a few muscle elements or one with a large number of muscle elements which is unable to arrive at a solution. For instance, in this study, the Delp model was constrained to 1 DOF at the knee and 2 DOF at the ankle in common with the original model and a number of other studies [8], [9], [16], [17]. These constraints were necessary to allow the optimisation to solve. In the case of the knee, although the Delp model provides 13 muscle elements that cross the joint there is insufficient variation in the moment arms of these elements to provide a solution when the model was unconstrained. The increased complexity of the Horsman muscle model provided sufficient variability in moment arms in 3-D to permit a solution without constraining the knee to 1 DOF.

This is clearly advantageous as these extra DOF may be particularly illuminating with regards to the mechanism of injury at the knee and for this reason the Horsman model may be preferred by future researchers interested in knee injuries. Equally, future work should explore the effect of constraining the DOF of the knee on the calculation of internal knee forces.

The performance of a 3-D model is highly influenced by the independence, variability and number of moment arms. These factors affect the degree of redundancy of the force sharing problem which in turn influences the ultimate solution. When the degree of redundancy is low (e.g. due to a small number of muscle elements) it is likely that most muscle elements will need to be involved in order to solve the force sharing problem. The interaction of these muscles with one another makes it likely that the overall level of activation will be relatively high. In contrast, when the degree of redundancy is higher, the combination of a larger solution set coupled with a decreased imperative for muscle interactions makes it likely that a solution will be found with a lower overall level of activation. In this study the use of the Horsman model resulted in a higher degree of redundancy than the Delp model, primarily as it consists of almost 4 times as many muscle elements. This meant that, even in the standing trial, the level of activation of the plantar-flexors was higher in the Delp model than the adjusted Horsman model, despite the fact that the Horsman ankle had an additional DOF. In high force activities, where the degree of redundancy is relatively small, the Delp model predicted markedly higher values. The patellofemoral joint contact force suggested by the Horsman model seems to be more reasonable when compared to previous findings [24], [41].

Complexity is a key issue in modelling. Increasingly complex models are not always advantageous as they can be more labour intensive to implement and interpret. This study demonstrates however, that in the given application the implementation of the more complex Horsman model rewarded the extra effort. For the activities considered the Horsman model provided a greater degree of redundancy than the model of Delp, and this resulted in patellofemoral joint contact force values more in line with those suggested by the previous literature. This demonstrates that the calculation of patellofemoral joint contact force by this type of methodology is clearly sensitive to the degree of redundancy of the chosen muscle model. As complex muscle models will tend to provide greater redundancy the complexity of the muscle model is therefore an important factor in ensuring a physiologically realistic solution.

In this study, the adjusted Horsman model predicted higher patellar tendon forces than the original Horsman model. However the two Horsman models suggested similar patellofemoral joint contact force values. This can be explained by the difference in the choice of patellofemoral joint model. The differing joint kinematics ameliorated the effect of higher patellar tendon forces on the patellofemoral joint contact force in the adjusted Horsman model. As the adjusted Horsman model represents the fairest comparison to the Delp model, it is apparent that the differences in forces caused by the varying complexity are greater than might be apparent if the Delp model was simply compared to the unadjusted Horsman model. This data also demonstrates the key role of the choice of patellofemoral joint model in determining patellofemoral joint contact force.

The Delp muscle model was created by amalgamating the results of previous work and does not represent an internally consistent data set. In contrast, the Horsman

muscle model is based upon the geometrical analysis of one cadaveric specimen. In addition, the Horsman muscle model comprises a much wider data set than that of Delp, including the position of bony anatomical landmarks and CORs. In the current study, the use of anatomical landmarks allowed a more accurate subject-specific scaling of the Horsman muscle model than was achievable using the Delp model. This demonstrates an advantage of more detailed muscle models over more simple implementations.

The performance of the Delp model at increasing hip flexion angles exemplifies the importance of physiologically realistic wrapping points. As the gluteal muscle elements are represented by straight line elements, as hip flexion angle increases the muscle lines of action pass to the flexion side of the COR. A more realistic model would wrap the muscle elements around the intervening structures constraining them to the extension side of the COR. Previous authors have refined the Delp model to include wrapping structures, however it is challenging to combine different anatomical data sets and therefore these structures may not be consistent with the derivation of the original Delp parameters (e.g. [16]) whereas the geometric primitives provided by Horsman are internally consistent with the rest of the data set. It is clearly imperative to choose a muscle model that is well defined in all joint ranges of motion. Although previous authors have modified Delp for this purpose, the existence of the Horsman muscle model may now make its employment a more attractive choice. This area is far from resolved, however, and future work should expand on the current literature exploring the key question of muscle wrapping [36], [42].

The results of this study demonstrate some of the considerations when employing muscle models in biomechanical analyses. A well posed muscle model must have sufficient independence, variability and number of muscle moment arms to ensure an adequate redundancy of the force sharing problem such that muscle forces are not overstated. Similarly, it is advantageous if the model allows ample redundancy to allow the study of at least 3 DOF at each joint, particularly if the application seeks to elucidate injury mechanisms. These considerations suggest that for any given application there may be a minimum degree of complexity necessary in order to arrive at a physiologically realistic solution. There are advantages to muscle models being derived from completely internally consistent data sets. The issue of correctly specifying the wrapping behaviour of muscles is of profound importance. With regards to the above considerations, the authors of this paper would therefore suggest that in many 3-D applications the Horsman muscle model would be preferred to the original model of Delp.

References

[1] **Arnold, A. S., Liu, M. Q., Schwartz, M. H., Ounpuu, S., Dias, L. S.,** and **Delp, S. L.** Do the hamstrings operate at increased muscle-tendon lengths and velocities after surgical lengthening? *J. Biomech.*, 2006, **39,** 1498-1506.

[2] **Charlton, I. W.,** and **Johnson, G. R.** A model for the prediction of forces at the glenohumeral joint. *Proc. IMechE Part H J. Eng. Med.*, 2006, **220(H),** 801-812.

[3] **Delp, S. L., Statler, K.,** and **Carroll, N. C.** Preserving plantar flexion strength after surgical-treatment for contracture of the triceps surae - a computer-simulation study. *J. Orthop. Res.*, 1995, **13,** 96-104.

[4] **Thelen, D. G., Chumanov, E. S., Best, T. M., Swanson, S. C.,** and **Heiderscheit, B. C.** Simulation of biceps femoris musculotendon mechanics during the swing phase of sprinting. *Med. Sci. Sport Exer.*, 2005a, **37,** 1931-1938.

[5] **Thelen, D. G., Chumanov, E. S., Hoerth, D. M., Best, T. M., Swanson, S. C., Young, M.,** and **Heiderscheit, B. C.** Hamstring muscle kinematics during treadmill sprinting. *Med. Sci. Sport Exer.*, 2005b, **37,** 108-114.

[6] **Thelen, D. G., Chumanov, E. S., Sherry, M. A.,** and **Heiderscheit, B. C.** Neuromusculoskeletal models provide insights into the mechanisms and rehabilitation of hamstring strains. *Exer. Sports Sci. Rev.*, 2006, **34,** 135-141.

[7] **van der Helm, F. C. T.,** and **Veeger, H. E. J.** Quasi-static analysis of muscle forces in the shoulder mechanism during wheelchair propulsion. *J. Biomech.*, 1996, **29,** 39-52.

[8] **Delp, S. L.** Surgery simulation: a computer graphics system to analyze and design musculoskeletal reconstructions of the lower limb. PhD thesis. Stanford University, 1990.

[9] **Delp, S. L., Loan, J. P., Hoy, M. G., Zajac, F. E., Topp, E. L.,** and **Rosen, J. M.** An interactive graphics-based model of the lower extremity to study orthopaedic surgical procedures. *IEEE Trans. Biomed. Eng.*, 1990, **37,** 757-767.

[10] **Delp, S. L.,** and **Loan, J. P.** A graphics-based software system to develop and analyze models of musculoskeletal structures. *Comp. Biol. Med.*, 1995, **25,** 21-34.

[11] **Arnold, A. S.,** and **Delp, S. L.** Rotational moment arms of the medial hamstrings and adductors vary with femoral geometry and limb position: implications of the treatment of internally rotated gait. *J. Biomech.*, 2001, **34,** 437-447.

[12] **Piazza, S. J.,** and **Delp, S. L.** The influence of muscles on knee flexion during the swing phase of gait. *J. Biomech.,* 1996, **29,** 723-733.

[13] **Brand, R. A., Peterson, I.,** and **Friederich, I.** The sensitivity of muscle force predictions to changes in physiologic cross-sectional area. *J. Biomech.,* 1986, **19,** 589-596.

[14] **Friederich, I.,** and **Brand, R. A.** Muscle fiber architecture in the human lower limb. *J. Biomech.,* 1990, **23,** 91-95.

[15] **Wickiewicz, T. L., Roy, R. R., Powell, P. L.,** and **Edgerton, V. R.** Muscle architecture of the human lower limb. *Clin. Orthop. Rel. Res.,* 1983, **179,** 275-283.

[16] **Anderson, F. C.,** and **Pandy, M. G.** A dynamic optimization solution for vertical jumping in three dimensions. *Comp. Meth. Biomech. Biomech. Eng.,* 1999, **2,** 201-231.

[17] **Nagano, A., Komura, T., Fukashiro, S.,** and **Himeno, R.,** Force, work and power output of lower limb muscles during human maximal-effort countermovement jumping. *J. Electromyog. Kinesiol.,* 2005, **15,** 367-376.

[18] **Horsman, M. D., Koopman, H. F. J. M., van der Helm, F. C. T., Poliacu Prose, L.,** and **Veeger, H. E. J.** Morphological muscle and joint parameters for musculoskeletal modelling of the lower extremity. *Clin. Biomech.,* 2007, **22,** 239-247.

[19] **Devereaux, M. D.,** and **Lachmann, S. M.** Patello-femoral arthralgia in athletes attending a sports injury clinic. *Brit. J. Sport Med.,* 1984, **18,** 18-21.

[20] **Brechter, J. H.,** and **Powers, C. M.** Patellofemoral joint stress during stair ascent and descent in persons with and without patellofemoral pain. *Gait Posture,* 2002a, **16**, 115-123.

[21] **Brechter, J. H.,** and **Powers, C. M.** Patellofemoral stress during walking in persons with and without patellofemoral pain. *Med. Sci. Sport Exer.,* 2002b, **34,** 1582-1593.

[22] **Feller, J. A., Amis, A. A., Andrish, J. T., Arendt, E. A., Erasmus, P. J.,** and **Powers, C. M.** Surgical biomechanics of the patellofemoral joint. *Arthrosc.,* 2007, **23,** 542-553.

[23] **Huberti, H. H.,** and **Hayes, W. C.,** Patellofemoral contact pressures: The influence of q-angle and tendofemoral contact. *J. Bone. Joint Surg. Am.,* 1984, **66-A,** 715-724.

[24] **Simpson, K. J., Jameson, E. G.,** and **Odum, S.** Estimated patellofemoral compressive forces and contact pressures during dance landings. *J. Appl. Biomech.*, 1996, **12,** 1-14.

[25] **Vanezis, A.,** and **Lees, A.** A biomechanical analysis of good and poor performers of the vertical jump. *Ergonomics*, 2005, **48**, 1594-1603.

[26] **Lees, A., Vanrenterghem, J.,** and **De Clercq, D.** The maximal and submaximal vertical jump: implications for strength and conditioning. *J. Streng. Cond. Res.*, 2004, **18**, 787-791.

[27] **Van Sint Jan, S.** Skeletal Landmark Definitions, guidelines for accurate and reproducible palpation. University of Brussels, Department of Anatomy (www.ulb.ac.be/~anatemb), 2005.

[28] **Van Sint Jan, S.,** and **Croce, U. D.** Identifying the location of human skeletal landmarks: why standardized definitions are necessary - a proposal. *Clin. Biomech.*, 2005, **20,** 659-660.

[29] **Horn, B. K. P.** Closed form solution of absolute orientation using unit quaternions. *J. Opt. Soc. Am.*, 1987, **4,** 629-642.

[30] **Lee, J.,** and **Shin, S. Y.** General construction of time-domain filters for orientation data. *IEEE Trans. Vis. Comp. Graphics*, 2002, **8,** 119-128.

[31] **Winter, D. A.** Biomechanics and motor control of human movement. Hoboken, NJ: John Wiley & Sons, 2005.

[32] **de Leva, P.** Adjustments to Zatsiorsky-Seluyanov's segment inertia parameters. *J. Biomech.*, 1996, **29,** 1223-1230.

[33] **Nisell, R., Nemeth, G.,** and **Ohlsen, H.** Joint forces in exension of the knee - analysis of a mechanical model. *Acta Orthop. Scand.*, 1986, **57,** 41-46.

[34] **van Eijden, T. M. G. J., Deboer, W.,** and **Weijs, W. A.** The orientation of the distal part of the quadriceps femoris muscle as a function of the knee flexion extension angle. *J. Biomech.*, 1985, **18,** 803-809.

[35] **Yamaguchi, G. T.,** and **Zajac, F. E.** A planar model for the knee-joint to characterize the knee extensor mechanism. *J. Biomech.*, 1989, **22,** 1-10.

[36] **Charlton, I. W.,** and **Johnson, G. R.** Application of spherical and cylindrical wrapping algorithms in a musculoskeletal model of the upper limb. *J. Biomech.*, 2001, **34,** 1209-1216.

[37] **Crowninshield, R. D.,** and **Brand, R. A.** A physiologically based criterion of muscle force prediction in locomotion. *J. Biomech.*, 1981, **14,** 793-801.

[38] **Yamaguchi, G. T.** Dynamic modeling of musculoskeletal motion: A vectorized approach for biomechanical analysis in three dimensions. New York: NY, Springer, 2001.

[39] **Powers, C. M., Chen, Y. J., Scher, I.,** and **Lee, T. Q.** The influence of patellofemoral joint contact geometry on the modeling of three dimensional patellofemoral joint forces. *J. Biomech.,* 2006, **39,** 2783-2791.

[40] **Wu, G., Siegler, S., Allard, P., Kirtley, C., Leardini, A., Rosenbaum, D., Whittle, M., Lima, D. D., Cristofolini, L.,** and **Witte, H.** ISB recommendation on definitions of joint coordinate system of various joints for the reporting of human joint motion--part I: ankle, hip, and spine. *J. Biomech.,* 2002, **35,** 543-548.

[41] **Smith, A. J.** Estimates of muscle and joint forces at the knee and ankle during a jumping activity. *J. Hum. Mov. Stud.*, 1975, **1**, 78-86.

[42] **Marsden, S. P.,** and **Swailes, D. C.** A novel approach to the calculation of musculotendon paths. *Proc. IMechE Part H J. Eng. Med.*, 2008, **222(H),** 51-61.

Tables

Figures

List of Notation

F	Objective function used in optimization
$\boldsymbol{l}$	Effective line of action of each muscle element
$\boldsymbol{r}$	Vector from COR to effective line of action of each muscle element
3-D	Three dimensional
COR	Centre of rotation
DOF	Degrees of freedom
F	Magnitude of individual muscle force
F_i	Intersegmental force
F_{max}	Magnitude of individual maximum muscle force
GCS	Global coordinate system
LCS	Local coordinate system
M_i	Intersegmental moment
n	Total number of muscle elements
$\boldsymbol{T}$	Torque created by each muscle about the COR
x	Anterior-posterior axis (positive values point anteriorly)
y	Superior-inferior axis (positive values point superiorly)
z	Lateral-medial axis (positive values point laterally)

Figure 1. Flow diagram illustrating the function of the model used in this study.

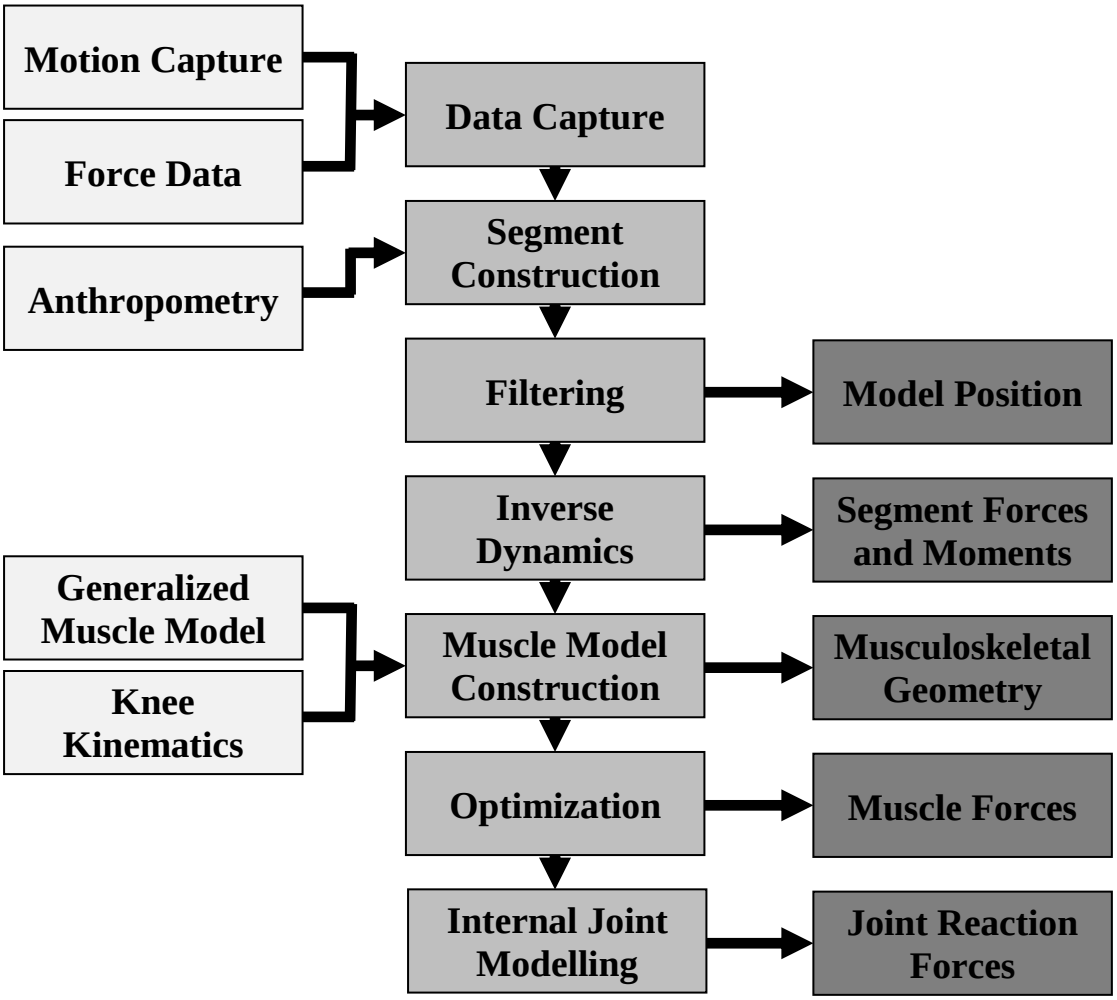

Figure 2. Construction of rigid linked segments representing the right lower limb.

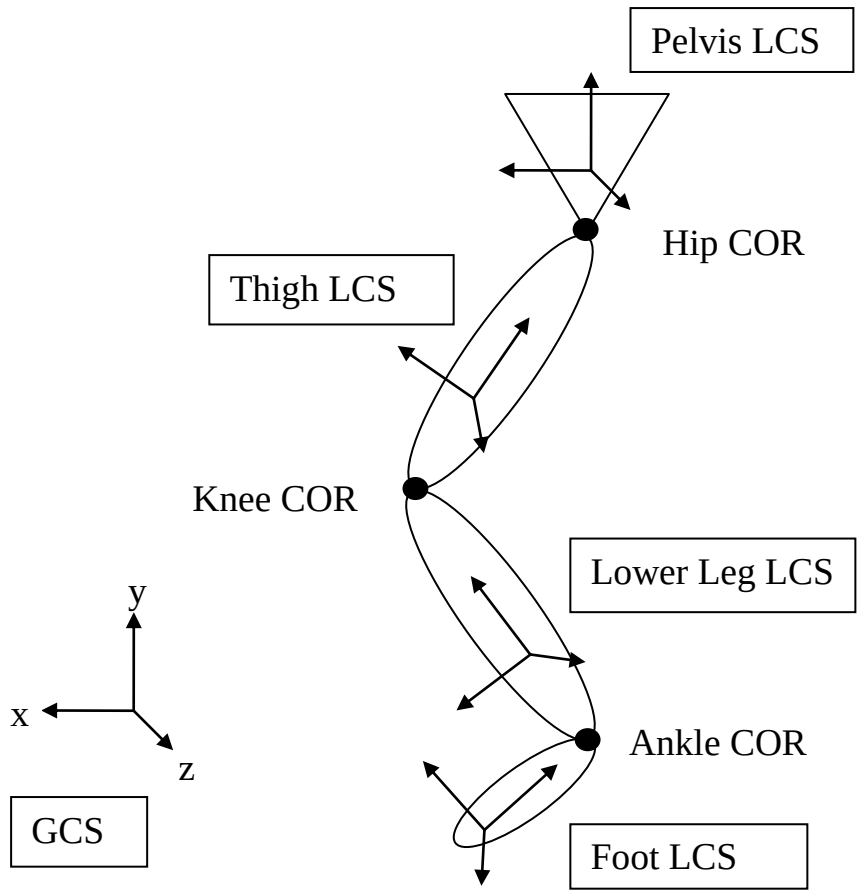

GCS – global coordinate system; LCS – local coordinate system; COR – centre of rotation

Figure 3. Inverse dynamics process.

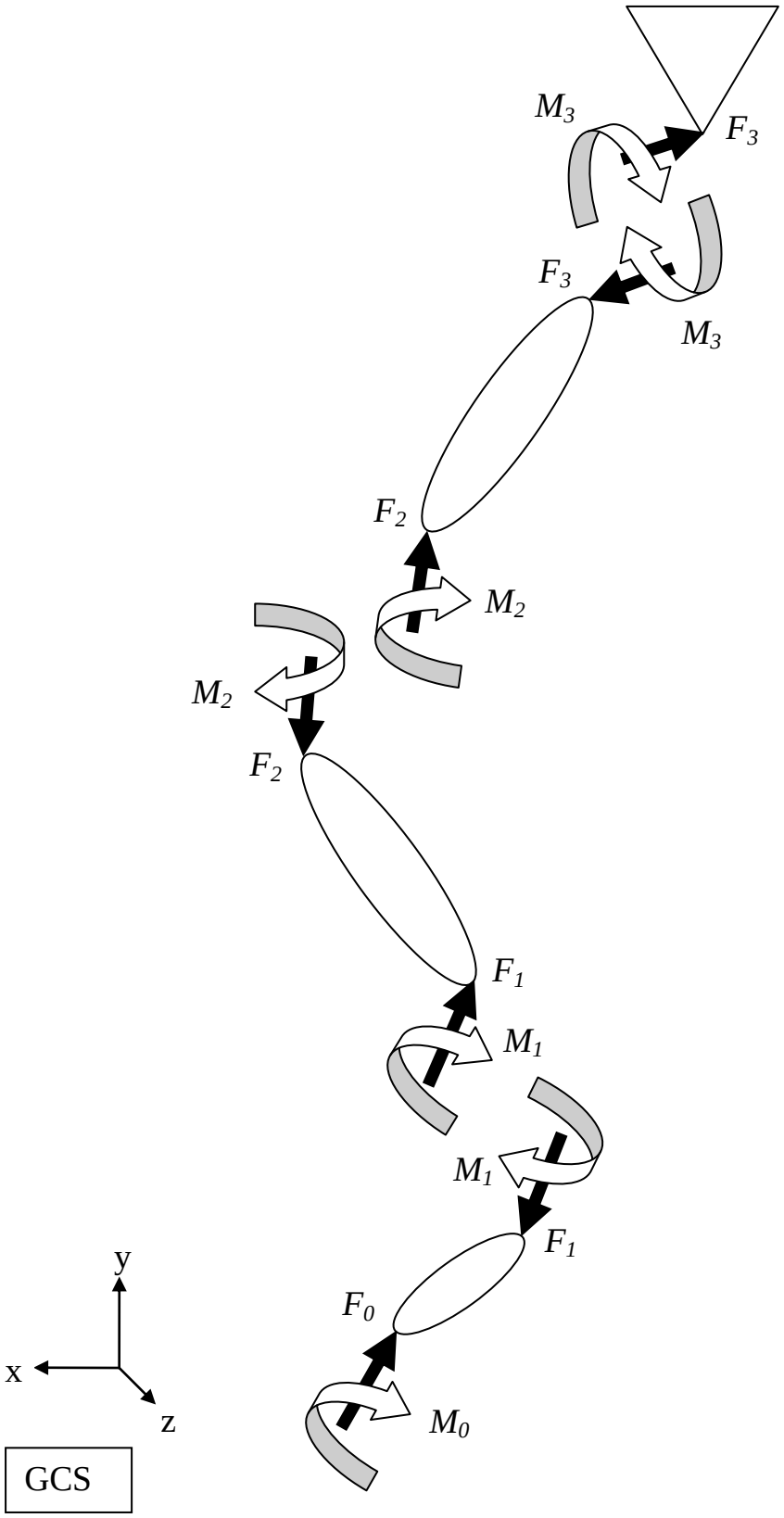

GCS – global coordinate system; F_i – intersegmental force; M_i – intersegmental moment

Figure

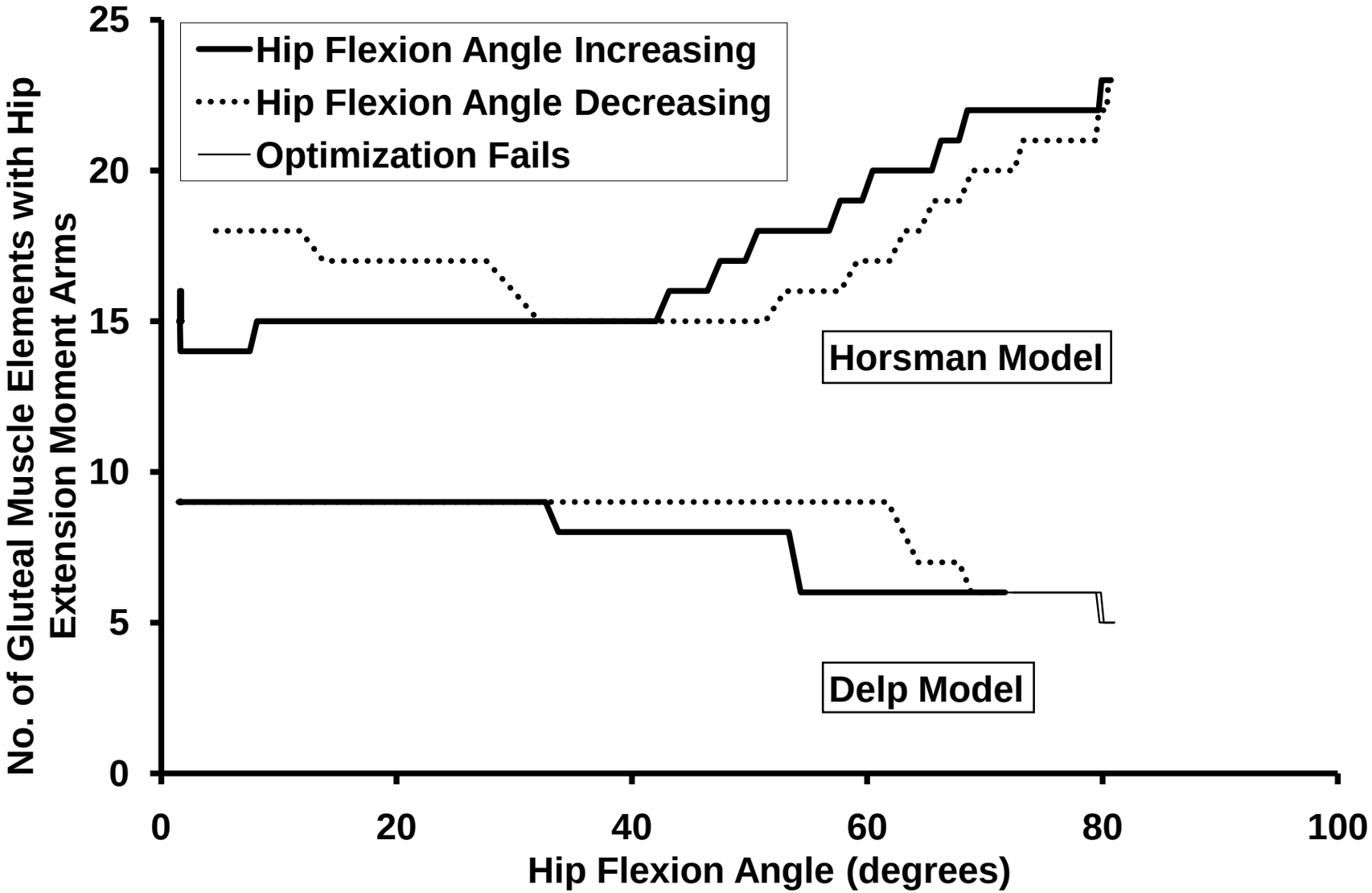
Hip Flexion Angle Increasing
Hip Flexion Angle Decreasing
Optimization Fails
Horsman Model
Delp Model
No. of Gluteal Muscle Elements with Hip Extension Moment Arms
Hip Flexion Angle (degrees)
0
5
10
15
20
25
0
20
40
60
80
100

Figure

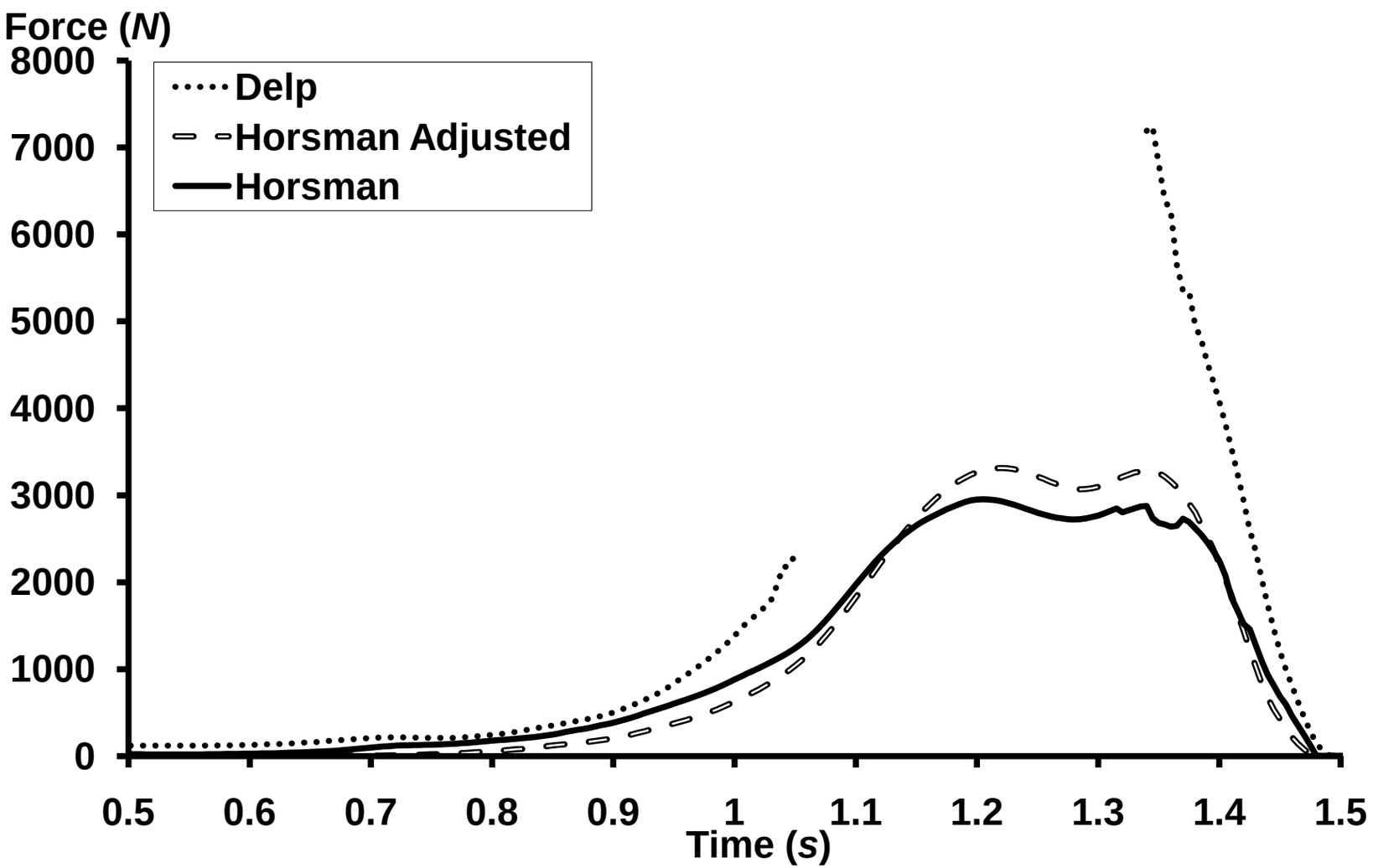
Force (N)
8000
7000
6000
5000
4000
3000
2000
1000
0
Delp
Horsman Adjusted
Horsman
0.5
0.6
0.7
0.8
0.9
1
1.1
1.2
1.3
1.4
1.5
Time (s)

Figure

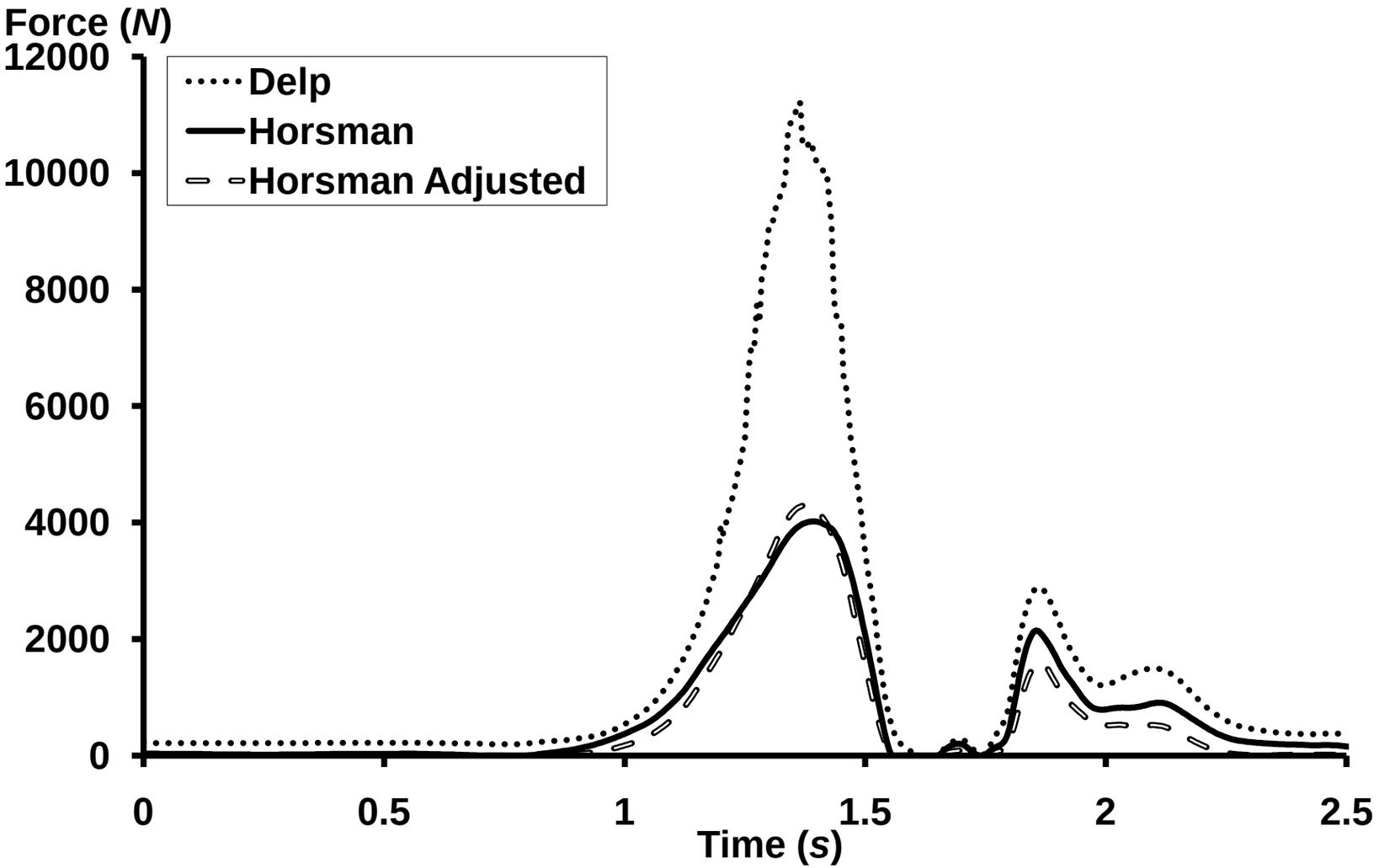
Force (N)
12000
10000
8000
6000
4000
2000
0
Delp
Horsman
Horsman Adjusted
0
0.5
1
1.5
2
2.5
Time (s)

Figure

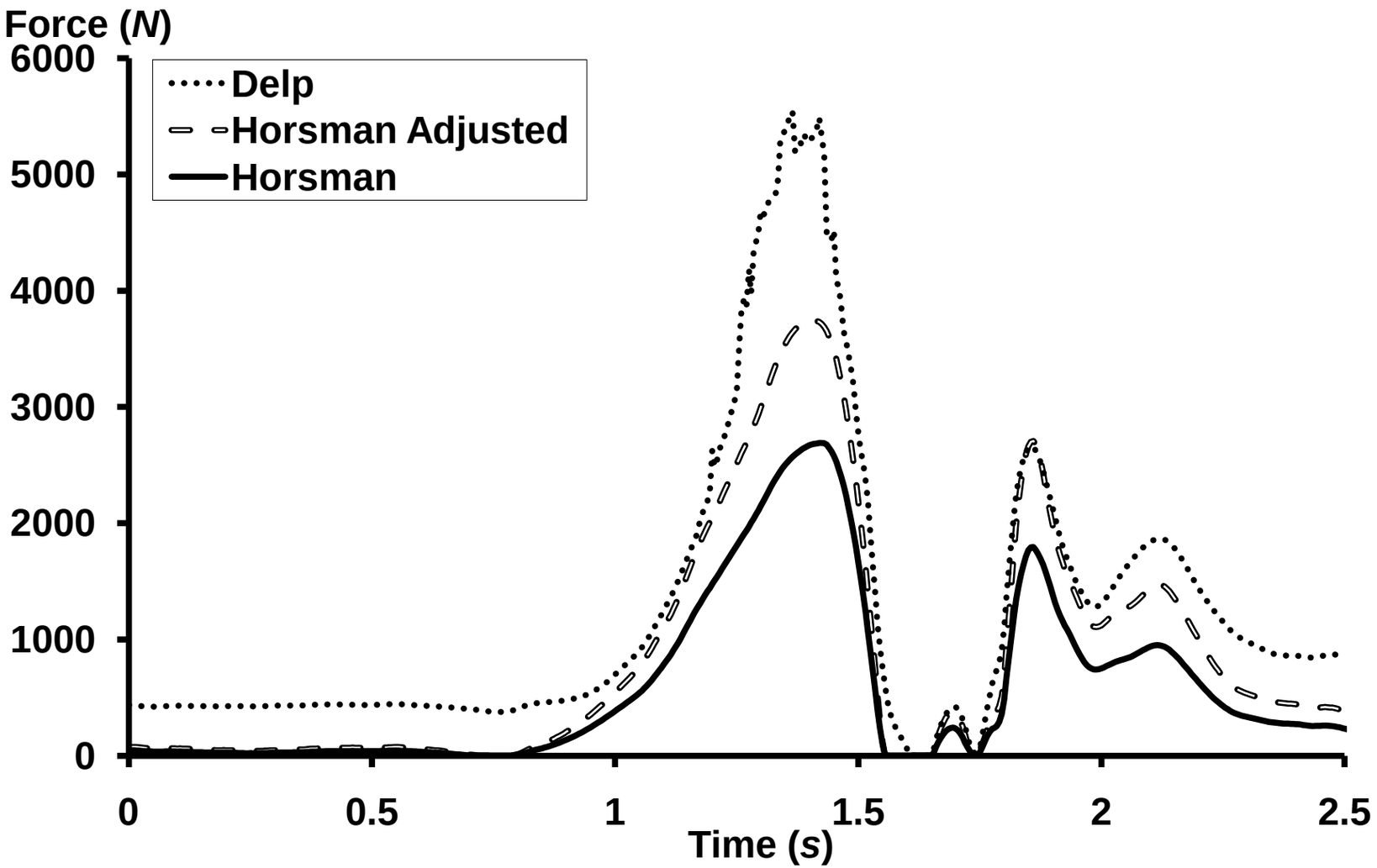
Force (N)
6000
5000
4000
3000
2000
1000
0
Delp
Horsman Adjusted
Horsman
0
0.5
1
1.5
2
2.5
Time (s)

Table 1. Muscle force in Newtons in standing as predicted by Delp and Horsman (adjusted) muscle models

Muscle Group	Delp	Horsman
Adductor Brevis	8	101
Adductor Longus	8	227
Adductor Magnus	30	0
Biceps Femoris (Long Head)	0	0
Biceps Femoris (Short Head)	0	14
Extensor Digitorum Longus	0	0
Extensor Hallucis Longus	0	0
Flexor Digitorum Longus	108	37
Flexor Hallucis Longus	131	0
Gastrocnemius (Lateral Head)	171	15
Gastrocnemius (Medial Head)	158	80
Gemellus	0	0
Gluteus Maximus	9	0
Gluteus Medius	0	152
Gluteus Minimus	0	8
Gracilis	7	12
Iliacus	0	0
Pectineus	4	47
Peroneus Brevis	0	5
Peroneus Longus	12	0
Peroneus Tertius	0	0
Piriformis	0	0
Psoas	0	10
Quadratus Femoris	2	0
Rectus Femoris	71	19
Sartorius	0	40
Semimembranosus	0	0
Semitendinosus	0	0
Soleus	199	288
Tensor Fascia Latae	11	36
Tibialis Anterior	0	36
Tibialis Posterior	111	132
Vastus Intermedius	74	0
Vastus Lateralis	74	0
Vastus Medialis	74	0

Table 2. Comparison of peak patellofemoral and patellar tendon forces during jumping and jerking (Horsman Model).

Peak Force (*kN*)	Jump		Jerk	
	Propulsive	Landing	Propulsive	Catching
Patellofemoral	3.0	3.4	4.0	2.1
Patellar Tendon	1.8	2.0	2.7	1.8